

Single top and Higgs associated production in the minimal $B - L$ model at the LHC

Bingfang Yang^{1,*} Zhiyong Liu^{1,†} Jinzhong Han^{2,‡} and Guang Yang^{3,§}

¹ *College of Physics & Electronic Engineering,
Henan Normal University, Xinxiang 453007, China*

² *School of Physics and Electromechanical Engineering,
Zhoukou Normal University, Henan, 466001, China*

³ *Basic Teaching Department, Jiaozuo University, Jiaozuo 454000, China*

(Dated: May 4, 2016)

Abstract

In this paper, we study the single top production in association with a Higgs boson in the $U(1)_{B-L}$ extension of the Standard Model at the LHC. We calculate the production cross sections of the processes $pp \rightarrow thX$ ($h = H_1, H_2; X = j, b, W$) in this model. Then we further study the observability of the process $pp \rightarrow tH_2j$ through $pp \rightarrow t(\rightarrow q\bar{q}'b)H_2(\rightarrow 4\ell)j$. We find that the systematic significance can be improved obviously, but it is still challenging for the 14 TeV LHC with high-luminosity to detect this signal.

PACS numbers: 14.65.Ha, 14.80.Ly, 11.30.Hv

*Electronic address: yangbingfang@htu.edu.cn

†Electronic address: 021168@htu.cn

‡Electronic address: hanjinzhong@zknv.edu.cn

§Electronic address: yxd5460@163.com

I. INTRODUCTION

In July 2012, a Higgs-like resonance with mass $m_h \sim 125$ GeV has been caught by the ATLAS and CMS experiments at the Large Hadron Collider (LHC)[1]. So far, all the measurements of the discovered new particle[2] are well compatible with the scalar boson predicted by the Standard Model(SM)[3].

It is well known that the SM cannot be the final theory of nature. Theoretically, successful explanation of some problems, such as the hierarchy problem, requires new physics beyond the SM near the TeV scale. Experimentally, the solid evidence for neutrino oscillation is one of the firm hints for new physics. The minimal extension of the SM is that the SM gauge groups are augmented by a $U(1)_{B-L}$ symmetry, where B and L represents the baryon number and lepton number respectively. The $B - L$ gauge symmetry can explain the presence of three right-handed neutrinos and provide a natural framework for the seesaw mechanism[4]. In addition, it's worth noting that $B - L$ symmetry breaking takes place at the TeV scale, hence giving rise to new and interesting TeV scale phenomenology.

Concerning the probe of new physics through the Higgs boson, the Yukawa couplings play an important role in probing the new physics. The top quark is the heaviest particle discovered and owns the strongest Yukawa coupling. The top quark Yukawa coupling is speculated to be sensitive to the electroweak symmetry breaking (EWSB) mechanism and new physics. The $t\bar{t}h$ production process is a golden channel for directly probing the top Yukawa coupling, however, this process cannot provide the information on the relative sign between the coupling of the Higgs to fermions and to vector bosons. As a beneficial supplement, the thj production process can bring a unique possibility[5] and many relevant works have been carried out[6].

The $U(1)_{B-L}$ model predicts heavy neutrinos, a TeV scale extra neutral gauge boson and an additional heavy neutral Higgs, which makes the model phenomenologically rich. The heavy Higgs state mixes with the SM Higgs boson so that some Higgs couplings are modified and this effect can also influence the process of single top and Higgs associated production. Besides, the process of single top and heavy Higgs associated production deserves attention, which is equally important for understanding the EWSB and probing new physics. By performing the detailed analysis on this process may provide a good opportunity to probe the $U(1)_{B-L}$ model signal.

The paper is structured as follows. In Sec.II we review the $U(1)_{B-L}$ model related to our work. In Sec.III we first calculate the production cross sections of the single top and $h(=H_1, H_2)$ associated production at the LHC, then explore the observability of t -channel process $pp \rightarrow tH_2j$ through $pp \rightarrow t(\rightarrow q\bar{q}'b)H_2(\rightarrow 4\ell)j$ by performing a parton-level simulation. Finally, we make a summary in Sec.IV.

II. A BRIEF REVIEW OF THE $U(1)_{B-L}$ MODEL

The minimal $B-L$ extension of the SM [7] is based on the gauge group $SU(3)_c \times SU(2)_L \times U(1)_Y \times U(1)_{B-L}$ with the classical conformal symmetry. Under this gauge symmetry, the invariance of the lagrangian implies the existence of a new gauge boson. In order to make the model free from all the gauge and gravitational anomalies, three generations of right-handed neutrinos are necessarily introduced.

In this model, the most general gauge-invariant and renormalisable scalar Lagrangian can be expressed as

$$\mathcal{L}_s = (D^\mu H)^\dagger D_\mu H + (D^\mu \chi)^\dagger (D_\mu \chi) - V(\chi, H), \quad (1)$$

with the scalar potential given by

$$V(\chi, H) = M_H^2 H^\dagger H + m_\chi^2 |\chi|^2 + \lambda_1 (H^\dagger H)^2 + \lambda_2 |\chi|^4 + \lambda_3 (H^\dagger H) |\chi|^2. \quad (2)$$

From the mass terms in the scalar potential, the mass matrix between the two Higgs bosons in the basis (H, χ) can be given by

$$M^2(H, \chi) = 2 \begin{pmatrix} \lambda_1 v^2 & \frac{\lambda_3}{2} vv' \\ \frac{\lambda_3}{2} vv' & \lambda_2 v'^2 \end{pmatrix}. \quad (3)$$

The mass eigenstates are related via the mixing matrix

$$\begin{pmatrix} H_1 \\ H_2 \end{pmatrix} = \begin{pmatrix} \cos \alpha & \sin \alpha \\ -\sin \alpha & \cos \alpha \end{pmatrix} \begin{pmatrix} H \\ \chi \end{pmatrix}, \quad (4)$$

where the mixing angle α ($-\frac{\pi}{2} < \alpha < \frac{\pi}{2}$) satisfies

$$\tan 2\alpha = \frac{\lambda_3 v' v}{(\lambda_2 v'^2 - \lambda_1 v^2)}. \quad (5)$$

The masses of the physical Higgs bosons H_1 and H_2 are given by

$$m_{H_1, H_2}^2 = \lambda_1 v^2 + \lambda_2 v'^2 \mp \sqrt{(\lambda_1 v^2 - \lambda_2 v'^2)^2 + (\lambda_3 v v')^2}, \quad (6)$$

where H_1 and H_2 are light SM-like and heavy Higgs bosons, respectively.

To complete the discussion on the Lagrangian, we write down the Yukawa term, which in addition to the SM terms has interactions involving the right-handed neutrinos N_R ,

$$\begin{aligned} \mathcal{L}_Y = & -y_{ij}^d \overline{(Q_L)_i} (d_R)_j H - y_{ij}^u \overline{(Q_L)_i} (u_R)_j \tilde{H} - y_{ij}^e \overline{(L_L)_i} (e_R)_j H \\ & - y_{ij}^\nu \overline{(L_L)_i} (N_R)_j \tilde{H} - y_{ij}^M \overline{(N_R)_i^c} (N_R)_j \chi + h.c., \end{aligned} \quad (7)$$

where $\tilde{H} = i\sigma^2 H^*$ and i, j runs from 1~3. The vacuum expectation value (VEV) of the χ field breaks the $B - L$ symmetry and generates the Majorana masses for the right handed neutrinos and the Dirac masses for the light neutrinos.

In terms of the mixing angle α , the couplings of H_1 and H_2 with the fermions and gauge bosons can be expressed as follows

$$\begin{aligned} H_1 f \bar{f} : & -\frac{e M_f \cos \alpha}{2 M_W s_W}, & H_2 f \bar{f} : & -\frac{e M_f \sin \alpha}{2 M_W s_W}, \\ H_1 W^+ W^- : & \frac{e M_W \cos \alpha}{s_W}, & H_2 W^+ W^- : & \frac{e M_W \sin \alpha}{s_W}, \\ H_1 Z Z : & \frac{e M_W \cos \alpha}{c_W^2 s_W}, & H_2 Z Z : & \frac{e M_W \sin \alpha}{c_W^2 s_W}. \end{aligned} \quad (8)$$

where f denotes the SM fermions, $s_W = \sin \theta_W$ with θ_W is the usual Weinberg angle.

III. NUMERICAL RESULTS AND DISCUSSIONS

For the single top and Higgs associated production, the three processes of interest are characterized by the virtuality of the W boson in the process[8]: (i) t -channel, where the W is spacelike; (ii) s -channel, where the W is timelike; (iii) W -associated production channel, where there is emission of a real W boson. In the $U(1)_{B-L}$ model, the lowest-order Feynman diagrams of the t -channel process $pp \rightarrow t H_1(H_2) j (j \neq b)$ are shown in Fig.1, the s -channel process $pp \rightarrow t H_1(H_2) \bar{b}$ are shown in Fig.2 and the W -associated production channel process $pp \rightarrow t H_1(H_2) W^-$ are shown in Fig.3. We can see that the Feynman diagrams for these processes are the same as the corresponding SM processes. Moreover, the conjugate processes where t is replaced by \bar{t} have been included in our calculations.

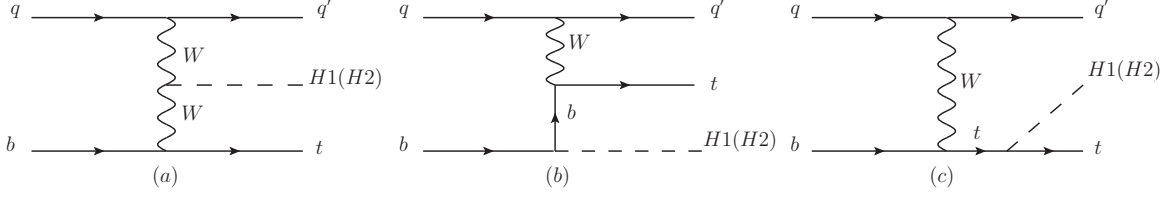


FIG. 1: Lowest-order Feynman diagrams for $pp \rightarrow tH_1(H_2)j$ in the $U(1)_{B-L}$ model.

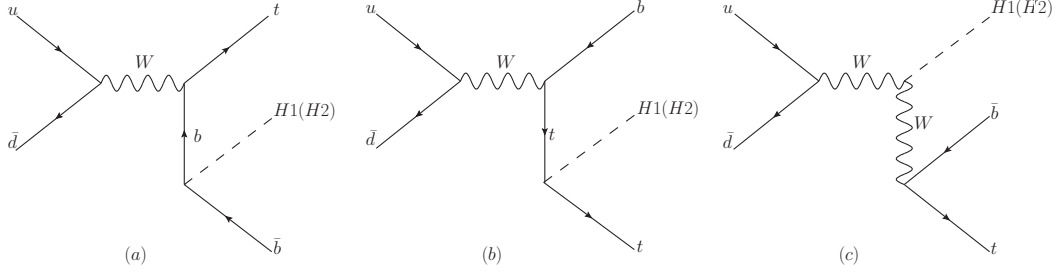


FIG. 2: Lowest-order Feynman diagrams for $pp \rightarrow tH_1(H_2)\bar{b}$ in the $U(1)_{B-L}$ model.

We compute the cross sections by using CalcHEP 3.6.25[9] with the parton distribution function CTEQ6L [10], and set the renormalization scale μ_R and factorization scale μ_F to be $\mu_R = \mu_F = (m_t + m_h + m_X)/2$, ($h = H_1, H_2$; $X = j, b, W$). The SM input parameters are taken as follows [11]:

$$\begin{aligned} m_t &= 173.2 \text{ GeV}, \quad m_Z = 91.1876 \text{ GeV}, \quad \alpha(m_Z) = 1/128, \\ \sin^2 \theta_W &= 0.231, \quad m_{H_1} = 125 \text{ GeV}, \quad \alpha_s(m_Z) = 0.1185. \end{aligned} \quad (9)$$

In our calculations, the relevant $U(1)_{B-L}$ model parameters are the mixing parameter α

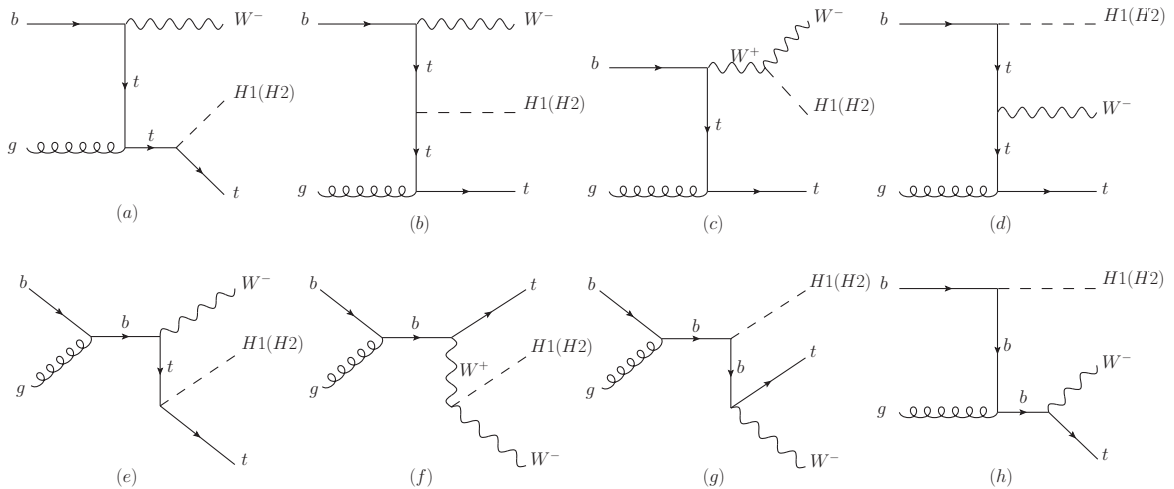


FIG. 3: Lowest-order Feynman diagrams for $pp \rightarrow tH_1(H_2)W^-$ in the $U(1)_{B-L}$ model.

and the heavy Higgs mass m_{H_2} . Considering the constraints in Refs.[12, 13], we choose the parameter space as follows: $0.01 < \sin \alpha < 0.4$, $250\text{GeV} \leq m_{H_2} \leq 1000\text{GeV}$.

A. Single top and H_1 associated production

In Fig.4, we show the production cross sections of the processes $pp \rightarrow tH_1j$, $pp \rightarrow tH_1\bar{b}$ and $pp \rightarrow tH_1W^-$ as a function of $\sin\alpha$ at the 8 and 14 TeV LHC in the $U(1)_{B-L}$ model, respectively. For clarity, we marked the corresponding SM process cross sections on the figures. We can see that the cross sections in the $U(1)_{B-L}$ model decrease with increasing $\sin\alpha$. Besides, the behavior of these three processes are similar for the 8 TeV and 14 TeV. This is easy to understand because there are the same change factor $\cos\alpha$ in the light Higgs H_1 couplings in Eq.(8) so that the production cross sections are suppressed by $\cos^2\alpha$, i.e., $\sigma_{B-L} = \sigma_{SM} \cos^2\alpha$. When $\sin\alpha \rightarrow 0$, the mixing between the light Higgs H_1 and the heavy Higgs H_2 will decouple so that the cross sections go back to the SM values.

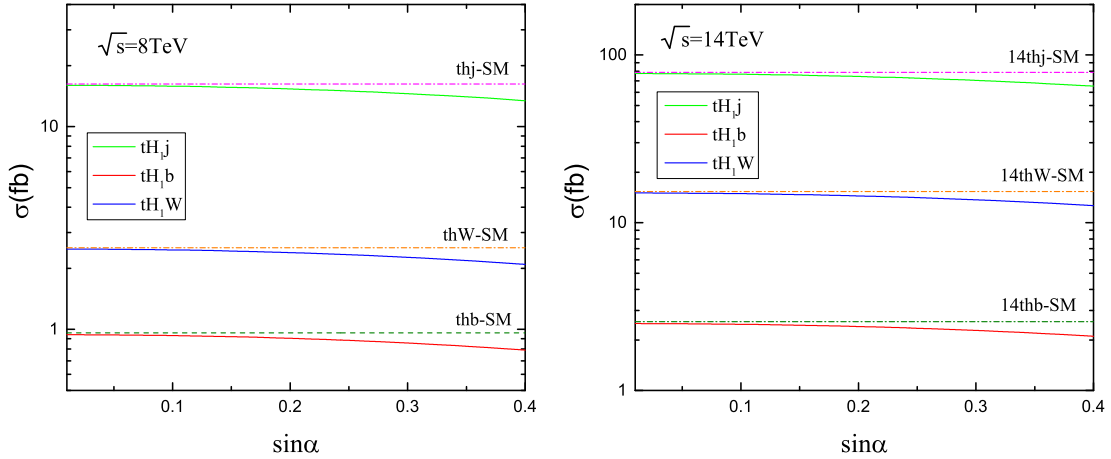


FIG. 4: The production cross sections σ_{tH_1j} , σ_{tH_1b} , σ_{tH_1W} as a function of $\sin\alpha$ at 8,14 TeV LHC in the $U(1)_{B-L}$ model.

B. Single top and H_2 associated production

In Figs.(5-6), we show the production cross sections of the processes $pp \rightarrow tH_2j$, $pp \rightarrow tH_2\bar{b}$ and $pp \rightarrow tH_2W^-$ as a function of $\sin\alpha$ at the 8 and 14 TeV LHC in the $U(1)_{B-L}$ model,

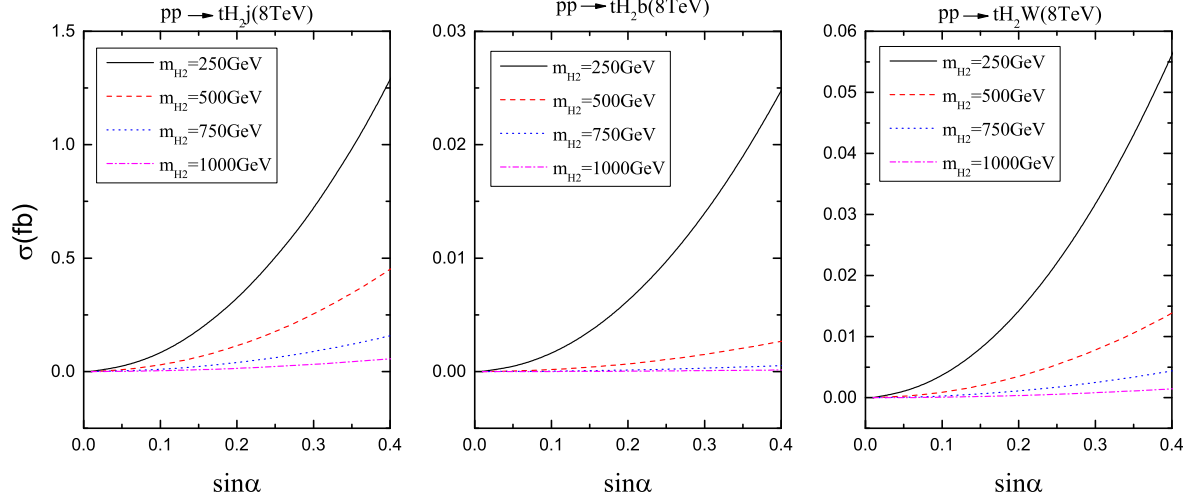


FIG. 5: The production cross sections $\sigma_{tH_2j}, \sigma_{tH_2b}, \sigma_{tH_2W}$ as a function of $\sin\alpha$ at 8 TeV LHC in the $U(1)_{B-L}$ model.

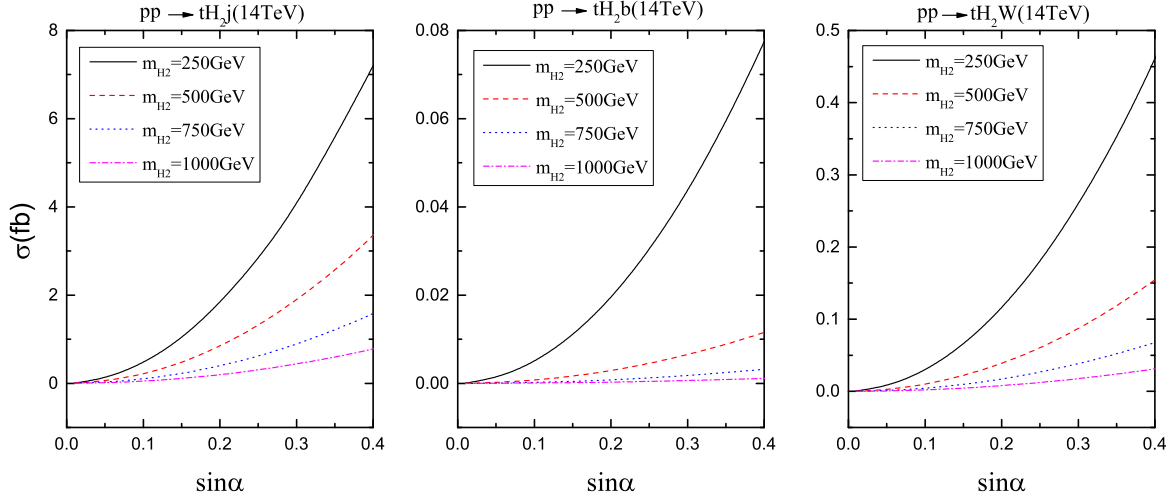


FIG. 6: The production cross sections $\sigma_{tH_2j}, \sigma_{tH_2b}, \sigma_{tH_2W}$ as a function of $\sin\alpha$ at 14 TeV LHC in the $U(1)_{B-L}$ model.

respectively. In order to see the influence of the heavy Higgs mass m_{H_2} on the production cross sections, we take $m_{H_2} = 250, 500, 750, 1000\text{GeV}$ as example. We can see that the cross sections increase with increasing $\sin\alpha$, which is because the heavy Higgs H_2 couplings in Eq.(8) are proportional to $\sin\alpha$ so that the cross sections are proportional to $\sin^2\alpha$.

C. Observability of $pp \rightarrow tH_2j$

The t -channel process dominates amongst these three production modes at the LHC, so we will explore the observability through the t -channel $pp \rightarrow tH_2j$ at 14 TeV LHC in the following section. The three most dominant decay modes of the heavy Higgs H_2 are WW, H_1H_1 and ZZ [14]. Though the branching fraction of $H_2 \rightarrow ZZ$ is smaller than the branching fractions of $H_2 \rightarrow WW$ and $H_2 \rightarrow H_1H_1$, the ZZ signal is much easier to separate from SM backgrounds. For the ZZ decay modes, the leptonic decay mode of ZZ offer the cleanest possible signatures though the di-jet and semi-leptonic decay modes of ZZ are larger. This leptonic decay mode has been studied in the heavy Higgs production at the LHC and it found that a heavy Higgs boson of mass smaller than 500 GeV can be discovered at the LHC with high-luminosity (HL-LHC)[13]. In our work, we concentrate on the channel $pp \rightarrow t(\rightarrow W^+b \rightarrow q\bar{q}'b)H_2(\rightarrow ZZ \rightarrow \ell_1^+\ell_1^-\ell_2^+\ell_2^-)j$ as shown in Fig.7, where H_2 decays to two Z bosons and the two Z bosons subsequently decay to four leptons. The signal is characterised by

$$3 \text{ jet} + b \text{ jet} + 4\ell \quad (10)$$

where j denotes the light jets and $\ell = e, \mu$. The largest background for this process comes from the $tZZj$ production mode that will generate the same final state.

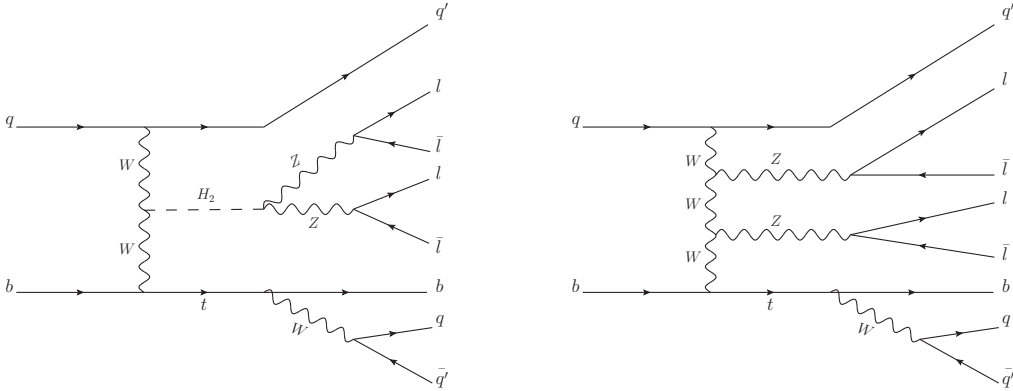


FIG. 7: Feynman diagrams for signal $pp \rightarrow tH_2j$ (Left) and background $pp \rightarrow tZZj$ (Right) including the decay chain with hadronic top quark, leptonic Z boson decay and Higgs decay $H_2 \rightarrow ZZ \rightarrow \ell_1^+\ell_1^-\ell_2^+\ell_2^-$ at the LHC.

We generate the signal and background events with with MadGraph5[15] and perform the parton shower and the fast detector simulations with PYTHIA[16] and Delphes[17]. To

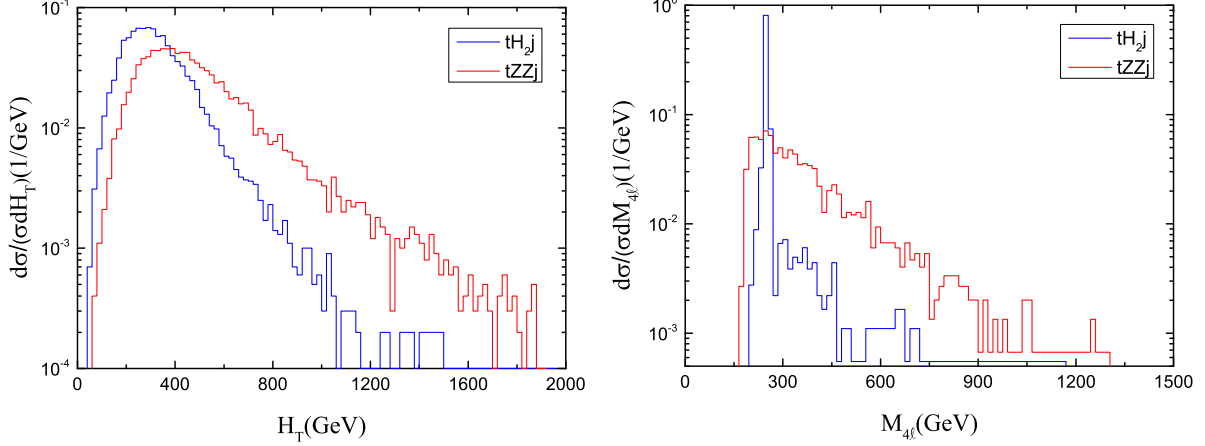


FIG. 8: The normalized distributions of $H_T, M_{4\ell}$ in the signal and background at 14 TeV LHC for $m_{H_2} = 250$ GeV, $\sin\alpha = 0.3$.

simulate b -tagging, we take moderate single b -tagging efficiency $\epsilon_b = 0.7$ for b -jet in the final state. Follow the analysis on $t\bar{t}h$ signature by ATLAS and CMS collaborations[18] at the LHC Run-I, the events are selected to satisfy the criteria as follows:

$$\begin{aligned}
\Delta R_{ik} &> 0.4, \quad i, k = b, j \text{ or } \ell \\
p_T^b &> 25 \text{ GeV}, \quad |\eta_b| < 2.5 \\
p_T^\ell &> 10 \text{ GeV}, \quad |\eta_\ell| < 2.5 \\
p_T^j &> 25 \text{ GeV}, \quad |\eta_j| < 5.
\end{aligned} \tag{11}$$

TABLE I: Cutflow of the cross sections for the signal and backgrounds at 14 TeV LHC on the benchmark point ($m_{H_2} = 250$ GeV, $\sin\alpha = 0.3$). All the conjugate processes of the signal and background have been included.

Cuts	$\sigma(\times 10^{-4}\text{fb})$		$\frac{S}{\sqrt{B}}$	$\frac{S}{B}$
	Signal	Background		
	tH_2j	$tZZj$	3000fb^{-1}	
No cuts	34.3	103.9	1.84	0.33
Basic cuts	15.6	50.2	1.20	0.31
$H_T < 380\text{GeV}$	11.3	19.5	1.40	0.58
$ M_{4\ell} - 250 < 20\text{GeV}$	2.97	1.04	1.60	2.86

Due to the small signal cross section, this process has a low signal-to-background ratio S/\sqrt{B} at the LHC. In this case, we will focus on enhancing the systematic significance S/B . Considering the transverse momentum of the leptons have little effect on the signal-to-background ratio and the systematic significance, we don't use them as selection cuts here. After analysis, we will adopt the following two cuts, the relevant normalized distributions of the kinematic variables for $m_{H_2} = 250$ GeV, $\sin\alpha = 0.3$ with respect to the background are shown in Fig.8.

Firstly, we impose the cut $H_T < 380$ GeV to separate signal from background, where $H_T (= \sum_{\text{hadronic particles}} ||\vec{p}_T||)$ is the total transverse hadronic energy. This cut can improve both the signal-to-background ratio S/\sqrt{B} and the systematic significance S/B .

After that, we apply the invariant mass of the four lepton system to further isolate the signal and let M_{4l} lie in the range $m_{H_2} \pm 20$ GeV. We can see that the signal-to-background ratio S/\sqrt{B} is improved and the systematic significance S/B is enhanced obviously.

The cut-flow cross sections of the signal and background for 14 TeV LHC are summarized in Table.I. After all cuts above, we can see that the systematic significance S/B is substantially improved. For the HL-LHC with a final integrated luminosity of $\mathcal{L} = 3000\text{fb}^{-1}$, the signal-to-background ratio S/\sqrt{B} can reach 1.6σ and systematic significance S/B can reach 2.86 for $m_{H_2} = 250$ GeV, $\sin\alpha = 0.3$. Unfortunatel, we can see that the number of signal events is very small because of the small leptonic branching ratio of the Z boson, which will be a trouble for detecting this signal at the LHC.

IV. SUMMARY

In the minimal $B-L$ extension of the SM, we investigated the single top and Higgs associated production at the LHC. We computed the production cross sections of the processes $pp \rightarrow tH_1(H_2)X (X = j, b, W)$ for 8, 14 TeV LHC and displayed the dependance of the cross sections on the relevant $U(1)_{B-L}$ model parameter. Moreover, we investigated the observability of process $pp \rightarrow tH_2j$ followed by the decays $t \rightarrow q\bar{q}'b$ and $H_2(\rightarrow ZZ \rightarrow \ell_1^+\ell_1^-\ell_2^+\ell_2^-)$ at 14 TeV LHC for $m_{H_2} = 250$ GeV, $\sin\alpha = 0.3$. We performed a simple parton-level simulation and found that it is challenging for the 14 TeV LHC and future HL-LHC with the integrated luminosity $\mathcal{L} = 3000\text{fb}^{-1}$ to observe the effect of the process $pp \rightarrow tH_2j$ through this final state. So, we have to expect a collider with higher energy and higher luminosity

to probe this effect. Maybe, a 100 TeV proton-proton collider with integrated luminosities of $3 \text{ ab}^{-1} \sim 30 \text{ ab}^{-1}$ can provide us a potential opportunity[19].

Acknowledgement

This work was supported by the National Natural Science Foundation of China (NNSFC) under grants No.11405047, the Startup Foundation for Doctors of Henan Normal University under Grant No.qd15207, the Joint Funds of the National Natural Science Foundation of China (U1404113), the Education Department Foundation of Henan Province(14A140010) , the Aid Project for the Mainstay Young Teachers in Henan Provincial Institutions of Higher Education of China(2014GGJS-283) and Colleges and universities in Henan province key scientific research project for 2016(16B140002).

-
- [1] G. Aad et al.(ATLAS Collaboration), Phys. Lett. B 710, 49 (2012); S. Chatrchyan et al.(CMS Collaboration), Phys. Lett. B 710, 26 (2012).
 - [2] G. Aad et al.(ATLAS Collaboration), Phys. Lett. B 726, 120 (2013), [arXiv:1307.1432]; Phys. Rev. D 90, 112015 (2014), [arXiv:1408.7084]; Phys. Rev. D 91, 012006 (2015), [arXiv:1408.5191]; JHEP 01, 069 (2015), [arXiv:1409.6212]; V. Khachatryan et al.(CMS Collaboration), Eur.Phys.J. C74, 3076 (2014), [arXiv:1407.0558]; S. Chatrchyan et al.(CMS Collaboration), Nature Phys. 10 (2014), [arXiv:1401.6527]; Phys. Rev. D 89, 092007 (2014), [arXiv:1312.5353]; JHEP 1401, 096 (2014), [arXiv:1312.1129].
 - [3] P. W. Higgs, Phys. Lett. 12, 132 (1964); P. W. Higgs, Phys. Rev. Lett. 13, 508 (1964); F. Englert and R. Brout, Phys. Rev. Lett. 13, 321 (1964); G. Guralnik, C. Hagen, and T. Kibble, Phys. Rev. Lett. 13, 585 (1964); T. Kibble, Phys.Rev. 155, 1554 (1967).
 - [4] S. Khalil, J. Phys. G 35, 055001 (2008); S. Khalil, Phys. Rev. D 82, 077702 (2010).
 - [5] G. Bordes and B. van Eijk, Phys. Lett. B 299, 315 (1993); A. Ballestrero and E. Maina, Phys. Lett. B 299, 312 (1993); W. J. Stirling and D. J. Summers, Phys. Lett. B 283, 411 (1992); J. L. Diaz-Cruz and O. A. Sampayo, Phys. Lett. B 276, 211 (1992).
 - [6] V. Barger, M. McCaskey, G. Shaughnessy, Phys. Rev. D 81, 034020 (2010), [arXiv:0911.1556]; M. Farina, C. Grojean, F. Maltoni, E. Salvioni and A. Thamm, JHEP 1305, 022 (2013),

- [arXiv:1211.3736]; L. Wu, JHEP 1502, 061 (2015), [arXiv:1407.6113]; A. Kobakhidze, L. Wu, J. Yue, JHEP 1410, 100 (2014), [arXiv:1406.1961]; A. Greljo, J. F. Kamenik and J. Kopp, JHEP 1407, 046 (2014), [arXiv:1404.1278]; S. Khatibi and M. M. Najafabadi, Phys. Rev. D 89, 054011 (2014), [arXiv:1402.3073]; D. Atwood, S. K. Gupta and A. Soni, JHEP 1410, 57 (2014), [arXiv:1305.2427]; Y. Wang, F. P. Huang, C. S. Li, B. H. Li, D. Y. Shao and J. Wang, Phys. Rev. D 86, 094014 (2012), [arXiv:1208.2902]; J. Chang, K. Cheung, J. S. Lee, C.-T. Lu, JHEP, 1405, 062 (2014), [arXiv:1403.2053]; B. F. Yang, J.Z. Han and N. Liu, JHEP 04, 148 (2015), [arXiv:1412.2927]; Y. M. Zhang and B. F. Yang, EPL 110, 21001 (2015); F. Demartin, F. Maltoni, K. Mawatari, M. Zaro, Eur. Phys. J. C 75, 267 (2015), [arXiv:1504.00611]; John Campbell, R. Keith Ellis, Raoul Röntsch, Phys. Rev. D 87, 114006 (2013).
- [7] R. N. Mohapatra and R. E. Marshak, Phys. Rev. Lett. 44, 1316 (1980); R. E. Marshak and R. N. Mohapatra, Phys. Lett. B 91, 222 (1980); C. Wetterich, Nucl. Phys. B 187, 343 (1981); A. Masiero, J. F. Nieves and T. Yanagida, Phys. Lett. B 116, 11 (1982); R. N. Mohapatra and G. Senjanovic, Phys. Rev. D 27, 254 (1983); W. Buchmuller, C. Greub and P. Minkowski, Phys. Lett. B 267, 395 (1991); L. Basso, A. Belyaev, S. Moretti, C. H. Shepherd-Themistocleous, Phys. Rev. D 80, 055030 (2009), [arXiv:0812.4313]; L. Basso, S. Moretti, G. M. Pruna, Phys. Rev. D 82, 055018 (2010), [arXiv:1004.3039].
- [8] F. Maltoni, K. Paul, T. Stelzer and S. Willenbrock, Phys. Rev. D 64, 094023 (2001), [hep-ph/0106293].
- [9] A. Belyaev, N. Christensen, A. Pukhov, Computer Physics Communications 184, 1729-1769 (2013), [arXiv:1207.6082].
- [10] J. Pumplin, D. R. Stump, J. Huston, H. L. Lai, P. M. Nadolsky and W. K. Tung, JHEP 0207, 012 (2002), [hep-ph/0201195].
- [11] K. A. Olive et al., (Particle Data Group), Chinese Physics C Vol. 38, No. 9, 090001 (2014).
- [12] T. Robens, T. Stefaniak, Eur. Phys. J. C 75, 104 (2015); L. Basso, S. Moretti, G. M. Pruna, JHEP 08, 122 (2011), [arXiv:1106.4762]; L. Basso, A. Belyaev, S. Moretti, G. M. Pruna, Phys. Rev. D 81, 095018 (2010), [arXiv:1002.1939].
- [13] S. Banerjee, M. Mitra, M. Spannowsky, Phys. Rev. D 92, 055013 (2015).
- [14] L. Basso, S. Moretti, G. M. Pruna, Phys. Rev. D 83, 055014 (2011), [arXiv:1011.2612].
- [15] J. Alwall et al., JHEP 1106, 128 (2011).
- [16] T. Sjostrand, S. Mrenna and P. Z. Skands, JHEP 0605, 026 (2006).

- [17] J. de Favereau, et al., JHEP 02, 057 (2014).
- [18] G. Aad et al. [ATLAS Collaboration], ATLAS-CONF-2012-135; S. Chatrchyan et al. [CMS Collaboration], CMS-PAS-HIG-12-025.
- [19] N. Arkani-Hamed, T. Han, M. Mangano, L.-T. Wang, arXiv:1511.06495 [hep-ph].